Fluid Antenna System Enhancing Orthogonal and Non-Orthogonal Multiple Access

Wee Kiat New, *Member, IEEE*, Kai-Kit Wong, *Fellow, IEEE*, Hao Xu, *Member, IEEE,* Kin-Fai Tong, *Fellow, IEEE*, Chan-Byoung Chae, *Fellow, IEEE*, *and* Yangyang Zhang

***Abstract*—Fluid antenna system (FAS) has recently emerged as a promising candidate for the sixth generation (6G) wireless networks. Unlike traditional antenna systems (TASs), FAS is a new wireless communication system where the so-called 'fluid' antenna (FA) can finely change its position within a given area. This unique ability allows FAS to harness additional diversity and multiplexing gains. In this letter, we investigate the applications of FAS in orthogonal multiple access (OMA) and non-orthogonal multiple access (NOMA) networks for performance enhancement. Specifically, we maximize the sum-rate of these multiple access schemes via optimal port selection and power allocation subject to per-user rate requirement. We then obtain the optimal variables in closed-form expressions. Our results reveal that FAS significantly improves the sum-rate of OMA and NOMA when compared to TAS. More interestingly, we discover that it is possible for FAS without channel state information at the transmitter (CSIT) to outperform optimal TAS with CSIT.**

***Index Terms*—6G, fluid antenna system, orthogonal multiple access, non-orthogonal multiple access.**

I. Introduction

Fluid antenna system (FAS) has recently emerged as a promising candidate for the sixth generation (6G) wireless networks which can also be incorporated with other promising applications such as reconfigurable intelligent surfaces, full-duplex communications, terahertz communications and many more. Fluid antenna (FA) refers to any software-controllable fluidic, conductive or dielectric structure that can change its position and shape to reconfigure the channel. Thus, FA includes all forms of movable and non-movable flexible antenna. Thanks to the advancement of using liquid metals, and RF switchable pixels for antennas, various FA prototypes have been developed by academia and industry in recent years [1], [2]. The most basic FA consists of one radio frequency (RF)-chain and N preset positions (known as ports) that are distributed in a given area.

Inspired by its flexibility and practicality, recent works in [3]–[6] have shown that FAS delivers promising rate and reliability in a point-to-point communication. Thus, extensions on multi-user communications have also been carried out. For instance, [7] proposed a novel scheme known as fluid antenna multiple access (FAMA) that could only be employed by FAS. The key principle of FAMA is to exploit spatial moments of deep fading to alleviate multi-user interference. Nevertheless, FAMA can only be applied when the interfering signals come from different antennas. Otherwise, other approaches are still required to mitigate the multi-user interference.

Existing wireless networks mostly rely on orthogonal multiple access (OMA) to serve multiple users. In OMA, multi-user interference is avoided by splitting the available degrees of freedom into orthogonal parts. However, this approach is not optimal when the channel state information at the transmitter (CSIT) is available. Instead, non-orthogonal multiple access (NOMA) that utilizes superposition coding and successive interference cancellation (SIC) can be more efficient than OMA. Specifically, NOMA is capacity-achieving in the broadcast channel and it has been proposed in the 6G wireless networks to support massive connectivity [8]. For instance, NOMA has been proposed for 6G use-cases such as space-aerial-terrestrial networks [9] and integrated sensing and communications [10]. However, the superiority of NOMA strongly depends on the SIC decoding order [11]. In particular, the signal of the weaker user must be first decoded/subtracted off before decoding the signal of the stronger user in the downlink and vice versa in the uplink. Hence, NOMA is no longer capacity-achieving if the CSIT is unavailable. In fact, it might be more efficient in some cases to allocate equal degrees of freedom and power allocation to the users when the CSIT is unavailable.

Recent studies have independently considered OMA and NOMA to accommodate multiple FAS receivers. In [12], the authors considered time-division multiple access (TDMA) and leveraged stochastic geometry to study the tradeoff between channel estimation and outage probability in large-scale cellular networks. Most recently, [13] considered space division multiple access in the uplink and minimized the total transmit power via receive beamforming, antenna positions of the base station and user power allocation subject to per-user rate requirement. These schemes are regarded as OMA. In contrast, [14] employed NOMA and derived the outage probability of the cooperative FAS receivers. Nonetheless, the impact of FAS on multiple access remains unclear even in the simplest case where the transmitter is equipped with a traditional antenna (TA) and the receivers are equipped with a single FA only.

Motivated by the above research gap, we investigate the impact of FAS in enhancing the performance of OMA and NOMA. The main contributions of this letter are summarized as follows. Firstly, we present a general FAS model that considers both OMA and NOMA to facilitate a fair comparison.

The work of W. K. New, K. K. Wong, H. Xu and K. F. Tong is supported by the Engineering and Physical Sciences Research Council (EPSRC) under Grant EP/W026813/1. The work of C. B. Chae is supported by the Institute of Information and Communication Technology Promotion (IITP) grant funded by the Ministry of Science and ICT (MSIT), Korea (No. 2021-0-02208, No. 2021-0-00486).

W. New (a.new@ucl.ac.uk), K. Wong (kai-kit.wong@ucl.ac.uk), H. Xu (hao.xu@ucl.ac.uk), and K. Tong (k.tong@ucl.ac.uk) are with the Department of Electronic and Electrical Engineering, University College London, London, WC1E 7JE, UK. K. Wong is also affiliated with Yonsei Frontier Lab., Yonsei University, Seoul 03722, Korea. C. Chae (cbchae@yonsei.ac.kr) is with the School of Integrated Technology, Yonsei University, Seoul 03722 Korea. Y. Zhang (yangyang.zhang@kuang-chi.org) is with Kuang-Chi Institute of Advanced Technology, Shenzhen 518100, China.

(Corresponding author: Kai-Kit Wong.)

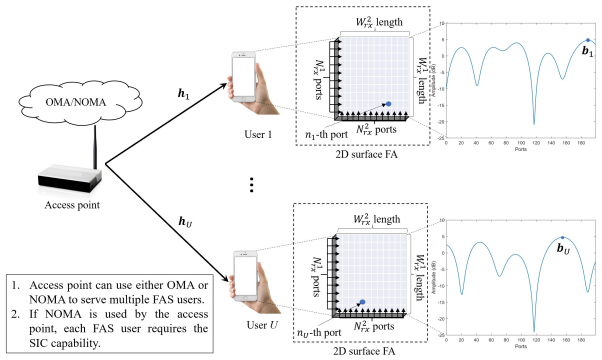

(a)

Figure 1: A schematic of an access point serving multiple FAS users in the downlink via OMA or NOMA.

Moreover, we consider a general scattering channel model that can be applied to various environments including line-of-sight (LOS) and non-LOS (NLOS) scenarios. Secondly, we formulate a non-convex optimization problem to maximize the sum-rate via optimal port selection and power allocation subject to per-user rate requirement. By exploiting the structure of the problems, we derive the optimal variables in closed-form expressions and show that optimizing OMA and NOMA in FAS can be straightforward in this setting. The time complexity is further presented. Thirdly, we study the sum-rate and individual rates of several benchmarking schemes across different parameters such as the signal-to-noise ratio (SNR), number of ports, area of the FA and number of users. We show that FAS provides a higher rate than TA system (TAS). More importantly, we demonstrate that it is possible for FAS without CSIT to outperform optimal TAS with CSIT. This highlights the unprecedented benefit of FAS over TAS.

II. System Model

As shown in Fig. 1, we consider an access point that is equipped with a single TA serving U FAS users in the downlink. Each FAS user is equipped with a single 2D surface FA that consists of $N_{\rm rx}$ preset locations (referred to as ports) that are distributed in an area of $W_{\rm rx}$. More concretely, we consider a grid structure where $N_{\rm rx}^i$ ports are uniformly distributed along a linear space of length $\lambda W_{\rm rx}^i$, where $i \in \{1,2\}$ and λ is the wavelength of the carrier frequency. Thus, we have $N_{\rm rx} = N_{\rm rx}^1 \times N_{\rm rx}^2$ and $W_{\rm rx} = \lambda^2 \left(W_{\rm rx}^1 \times W_{\rm rx}^2\right)$. Furthermore, we introduce an appropriate mapping function so that $f_0\left(n_u\right) = \left(n_u^1, n_u^2\right)$ and $f_0^{-1}\left(n_u^1, n_u^2\right) = n_u$ where $n_u \in \{1,\ldots,N_{\rm rx}\}$, $n_u^1 \in \left\{1,\ldots,N_{\rm rx}^1\right\}$ and $n_u^2 \in \left\{1,\ldots,N_{\rm rx}^2\right\}$.

The complex channels from the access point to user u can be modeled as [15]

$$\boldsymbol{h}_u = \sqrt{\frac{K}{K+1}} e^{j\omega_{t,u}} \boldsymbol{a}_r\left(\theta_{0,r}^{t,u}, \phi_{0,r}^{t,u}\right) + \sqrt{\frac{1}{L}} \sqrt{\frac{1}{K+1}} \sum_{l=1}^{L} \kappa_l^{t,u} \boldsymbol{a}_r\left(\theta_{l,r}^{t,u}, \phi_{l,r}^{t,u}\right), \quad (1)$$

in which K denotes the Rice factor, $\omega_{t,u}$ is the phase of the LOS component, $\kappa_l^{t,u}$ is the complex channel coefficient of the l-th scattered component and L is the number of NLOS paths.[1] Furthermore, $\boldsymbol{a}_r\left(\theta_{l,r}^{t,u}, \phi_{l,r}^{t,u}\right)$ is the receive steering vector which is given by [15]

$$\boldsymbol{a}_r\left(\theta_r, \phi_r\right) = \left[\begin{array}{cccc} 1 & e^{\frac{j2\pi W_{\rm rx}^2 \sin\theta_r \cos\phi_r}{N_2^{\rm rx}-1}} & \ldots & e^{j2\pi W_{\rm rx}^2 \sin\theta_r \cos\phi_r} \end{array}\right]^T \otimes \left[\begin{array}{cccc} 1 & e^{\frac{j2\pi W_{\rm rx}^1 \sin\phi_r}{N_1^{\rm rx}-1}} & \ldots & e^{j2\pi W_{\rm rx}^1 \sin\phi_r} \end{array}\right]^T, \quad (2)$$

where $\otimes$ is the Kronecker tensor product, $(\cdot)^T$ is the transpose operator, and θ_r and ϕ_r are the azimuth and elevation angle-of-arrival, respectively. It is worth noting that if $L \to \infty$ and $K > 0$, the magnitude of each entry of $\boldsymbol{h}_u$ follows Ricean fading. On the other hand, if $K = 0$ and $L \to \infty$, the magnitude of each entry of $\boldsymbol{h}_u$ follows Rayleigh fading.

In the Rayleigh fading case, the covariance between the n_u-th and $\tilde{n}_u$-th ports at the user is derived as [6]

$$\varrho_{n_u,\tilde{n}_u} = \Omega_u \mathcal{J}_0\left(2\pi \sqrt{\left(\frac{n_u^1 - \tilde{n}_u^1}{N_1^{\rm rx}-1} W_{\rm rx}^1\right)^2 + \left(\frac{n_u^2 - \tilde{n}_u^2}{N_2^{\rm rx}-1} W_{\rm rx}^2\right)^2}\right), \quad (3)$$

where Ω_u is the variance of the entry of $\boldsymbol{h}_u$. In (3), $\mathcal{J}_0\left(\cdot\right)$ is the spherical Bessel function of the first kind. Unlike TAS, it is worth highlighting that in FAS, we can have $\varrho_{n_u,\tilde{n}_u} = \Omega_u$ as $N_{\rm rx} \to \infty$ for some n_u and $\tilde{n}_u$.

Since each user can only switch its FA to a specific position (i.e., activates a port), the received signal of user u is

$$y_u = \boldsymbol{b}_u^T\left(\boldsymbol{h}_u x + \boldsymbol{\eta}_u\right), \quad (4)$$

where $\boldsymbol{b}_u = \left[b_u^1, \ldots, b_u^{N_{\rm rx}}\right]^T \in \mathcal{E} = \{\boldsymbol{e}_1, \ldots, \boldsymbol{e}_{N_{\rm rx}}\}$ and $\boldsymbol{e}_n$ represents an all-zero vector except the n-th entry being unity. In (4), $x = \sum_{\tilde{u}=1}^{U} s_{\tilde{u}}$ where $s_{\tilde{u}}$ is the signal of user $\tilde{u}$ with zero mean and variance of P and $\boldsymbol{\eta}_u$ is the additive white Gaussian noise vector of user u with zero mean and covariance of $N_0\boldsymbol{I}$, where $\boldsymbol{I}$ is the identity matrix.[2]

Next, we apply FAS to OMA which we refer to as FAS-OMA. In FAS-OMA, we consider a practical scheme where $\frac{1}{U}$ degree of freedom is given to each user (e.g., TDMA). The achievable rate of user u can be derived as

$$R_u^{\rm OMA} = \frac{1}{U} \log\left(1 + \alpha_u U {\rm SNR} \left|\boldsymbol{b}_u^T \boldsymbol{h}_u\right|^2\right), \quad (5)$$

where ${\rm SNR} = \frac{P}{N_0}$ and α_u is the fraction of power allocated to user u such that $\sum_{\forall u} \alpha_u = 1$.

Similarly, FAS can be applied to NOMA which we refer to as FAS-NOMA. In FAS-NOMA, the optimal decoding strategy is to perform SIC based on user signal strengths. To facilitate this, we assume that $\left|\boldsymbol{b}_1^T \boldsymbol{h}_1\right|^2 \geq \ldots \geq \left|\boldsymbol{b}_U^T \boldsymbol{h}_U\right|^2$. This suggests that the k-th user must first decode its signal and treat the l-th user's signal as noise where $k > l$. Using this optimal decoding strategy, the achievable rate of user u can be derived as[3]

$$R_u^{\rm NOMA} = \log\left(1 + \frac{\beta_u {\rm SNR} \left|\boldsymbol{b}_u^T \boldsymbol{h}_u\right|^2}{\sum_{w<u} \beta_w {\rm SNR} \left|\boldsymbol{b}_u^T \boldsymbol{h}_u\right|^2 + 1}\right), \quad (6)$$

[1] Note that only a small number of observed ports is required to obtain the full channel state information of (1) due to the strong spatial correlation [16].

[2] Compared to TAS, no additional interference is introduced in FAS.

[3] Since NOMA is capacity-achieving in this setup, rate-splitting multiple access (RSMA) is not considered.

where $\sum_{\forall u}\beta_u = 1$. It is worth pointing out that if $\boldsymbol{b}_u, \forall u$ is fixed, then FAS-NOMA and FAS-OMA are reduced to the traditional NOMA (TAS-NOMA) and traditional OMA (TAS-OMA), respectively.[4] For benchmarking, we also consider the case where each user randomly selects $\boldsymbol{b}_u$ from $\mathcal{E}$. In such cases, FAS-NOMA and FAS-OMA are referred to as RAS-NOMA and RAS-OMA, respectively.

III. Optimization, Feasibility and Complexity

In this section, we aim to maximize the sum-rate of FAS-OMA and FAS-NOMA via optimal port selection and power allocation subject to per-user rate requirement. To this end, we exploit the structure of the problems to obtain the optimal variables in closed-form expressions. In FAS-OMA, the optimization problem is formulated as

$$\max_{\boldsymbol{b}_u,\forall u,\boldsymbol{\alpha}} \quad \sum_{u=1}^{U} R_u^{\mathrm{OMA}} \tag{7a}$$

$$\text{s.t.} \quad R_u^{\mathrm{OMA}} \geq R_{\min}, \forall u, \tag{7b}$$

$$\boldsymbol{\alpha}^T\mathbf{1} = 1, \tag{7c}$$

where $\boldsymbol{\alpha} = [\alpha_1 \dots \alpha_U]^T$ and $\mathbf{1}$ is the all-one vector. Although the optimization variables are mutually coupled, it can be verified that the optimal $\boldsymbol{b}_u^*, \forall u$, is $\boldsymbol{e}_{n^*}$ where the n^*-th entry of $|\boldsymbol{h}_u|^2$ is the largest. This is because, for any $a_u \geq 0$, we have the following property

$$\frac{1}{U}\log\left(1+\alpha_u U\mathrm{SNR}\left|\boldsymbol{b}_u^T\boldsymbol{h}_u\right|^2\right) \leq \frac{1}{U}\log\left(1+\alpha_u U\mathrm{SNR}\left|\boldsymbol{b}_u^{*^T}\boldsymbol{h}_u\right|^2\right). \tag{8}$$

Thus, (7) can be simplified to

$$\max_{\boldsymbol{\alpha}} \quad \sum_{u=1}^{U}\frac{1}{U}\log\left(1+\alpha_u U\mathrm{SNR}\left|\boldsymbol{b}_u^{*^T}\boldsymbol{h}_u\right|^2\right), \tag{9a}$$

$$\text{s.t.} \quad \frac{1}{U}\log\left(1+\alpha_u U\mathrm{SNR}\left|\boldsymbol{b}_u^{*^T}\boldsymbol{h}_u\right|^2\right) \geq R_{\min}, \forall u, \tag{9b}$$

$$\boldsymbol{\alpha}^T\mathbf{1} = 1, \tag{9c}$$

which is a standard waterfilling problem. By investigating the dual problem of (9), we can obtain the closed-form solution where $\alpha_u^* = \max\left\{\frac{1}{\nu^*} - \frac{1}{g_u}, c_u\right\}$, $c_u = \frac{2^{UR_{\min}}-1}{U\mathrm{SNR}\left|\boldsymbol{b}_u^{*^T}\boldsymbol{h}_u\right|^2}$ and $g_u = U\mathrm{SNR}\left|\boldsymbol{b}_u^{*^T}\boldsymbol{h}_u\right|^2$. Concretely, ν^* can be obtained using the bisection method so that $\sum_{u=1}^{U}\alpha_u^* = 1$. It can be verified that (9) is an infeasible problem if $\sum_{u=1}^{U} c_u > 1$. If the CSIT is unavailable, the access point can allocate equal power allocation to all OMA users. We refer to this scheme as FAS-OMAR. If $\boldsymbol{b}_u$ is fixed, FAS-OMAR is reduced to TAS-OMAR.

[4]In terms of implementation, the access point of FAS needs to allocate N_p pilot symbols to each user to obtain the CSIT where $1 < N_p \ll N_{\mathrm{rx}}$ and each FAS user needs to find the optimal port $\boldsymbol{b}_u^*$ from N_{rx} ports. Compared to TAS-NOMA, no additional SIC complexity is introduced in FAS-NOMA since the u-th user similarly needs to perform SIC $(U-u)$ times.

In FAS-NOMA, the optimization problem is formulated as

$$\max_{\boldsymbol{b}_u,\forall u,\boldsymbol{\beta}} \quad \sum_{u=1}^{U} R_u^{\mathrm{NOMA}} \tag{10a}$$

$$\text{s.t.} \quad R_u^{\mathrm{NOMA}} \geq R_{\min}, \forall u, \tag{10b}$$

$$\boldsymbol{\beta}^T\mathbf{1} = 1, \tag{10c}$$

where $\boldsymbol{\beta} = [\beta_1 \dots \beta_U]^T$. In general, (10) is a non-convex optimization problem. By exploiting the fact that $\log\left(1+\frac{k_0 c_0}{\sum_u k_u c_0 + 1}\right)$ is monotonically increasing with respect to (w.r.t.) to c_0, it can be verified that the optimal $\boldsymbol{b}_u^*, \forall u$, is also $\boldsymbol{e}_{n^*}$. Thus, (10) can be reduced to

$$\max_{\boldsymbol{\beta}} \sum_{u=1}^{U}\log\left(1+\frac{\beta_u\mathrm{SNR}\left|\boldsymbol{b}_u^{*^T}\boldsymbol{h}_u\right|^2}{\sum_{w<u}\beta_w\mathrm{SNR}\left|\boldsymbol{b}_u^{*^T}\boldsymbol{h}_u\right|^2+1}\right) \tag{11a}$$

$$\text{s.t.}\log\left(1+\frac{\beta_u\mathrm{SNR}\left|\boldsymbol{b}_u^{*^T}\boldsymbol{h}_u\right|^2}{\sum_{w<u}\beta_w\mathrm{SNR}\left|\boldsymbol{b}_u^{*^T}\boldsymbol{h}_u\right|^2+1}\right) \geq R_{\min}, \forall u, \tag{11b}$$

$$\boldsymbol{\beta}^T\mathbf{1} = 1, \tag{11c}$$

which is a standard downlink sum-rate NOMA problem. As a consequence, we can obtain the closed-form solution by using the same line of argument as in [11]. In particular, we have $\beta_u^* = \left(2^{R_{\min}}-1\right)\left(\sum_{w<u}\beta_w^* + f_u\right), \forall u > 1$, $\beta_1^* = \left(2^{R_{\min}}-1\right)f_1 + \mu^*$ and $f_u = \frac{1}{\mathrm{SNR}\left|\boldsymbol{b}_u^{*^T}\boldsymbol{h}_u\right|^2}$. In this solution, μ^* can be obtained using the bisection method so that $\sum_{u=1}^{U}\beta_u^* = 1$. By investigating the minimum power to satisfy the per-user rate requirement, it can be confirmed that (11) is an infeasible problem if $\sum_{u=0}^{U-1}\frac{2^{uR_{\min}}}{\mathrm{SNR}\left|\boldsymbol{b}_{U-u}^{*^T}\boldsymbol{h}_{U-u}\right|^2} > \frac{1}{\left(2^{R_{\min}}-1\right)}$.

Since the access point needs to obtain the optimal power allocation using bisection and each user needs to find the optimal port $\boldsymbol{b}_u^*$ from N_{rx} ports, the time complexity to compute optimal FAS-OMA and FAS-NOMA is $\mathcal{O}\left(\epsilon_0 + UN_{\mathrm{rx}}\right)$ where ϵ_0 is the tolerance level for the bisection method.

IV. Results and Discussions

In this section, we present the simulation results to compare the performance of FAS and TAS. Unless stated otherwise, we assume that $K = 0$, $L = 50$, $\Omega_u = 1, \forall u$, $\mathrm{SNR} = 30\mathrm{dB}$, $W_{\mathrm{rx}} = 2\lambda \times 1\lambda$, $N_{\mathrm{rx}} = 20 \times 10$, $R_{\min} = 1\mathrm{bps/Hz}$ and $U = 4$. In TAS, we assume that $\boldsymbol{b}_u = [1, 0, \dots, 0]^T, \forall u$. The power allocation of these schemes is optimized accordingly.

In Fig. 2, we present the sum-rate of different schemes over different values of SNR. As it is seen, FAS-NOMA has the highest sum-rate followed by FAS-OMA, FAS-OMAR, TAS-NOMA, TAS-OMA and TAS-OMAR. This shows that FAS without CSIT (i.e., FAS-OMAR) can outperform optimal TAS with CSIT (i.e., TAS-NOMA). The rationale behind the performance improvement of FAS over TAS is that FAS user can find a more desirable channel in the spatial domain while TAS user has no such flexibility. Nevertheless, there is a limit to how much rate can be improved in FAS.

When compared to the same type of multiple access, RAS has the same sum-rate as TAS which implies that the random

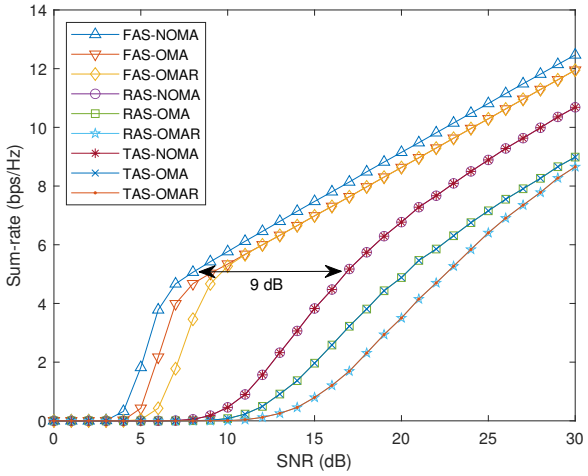

Figure 2: Sum-rate against different values of SNR.

port selection in FAS does not cause harm in this setting. In the high SNR regime, FAS-OMA and FAS-OMAR achieve similar sum-rates because the capacity of waterfilling power allocation approaches to that of equal power allocation as the SNR increases. However, in the medium/low SNR regimes, the sum-rate of FAS-OMA is strictly higher than that of FAS-OMAR since the power allocation plays a vital role in improving the sum-rate. To achieve a specific sum-rate, FAS requires less SNR than TAS. For instance, FAS-NOMA requires only 8 dB while TAS-NOMA requires 17 dB (i.e., a 9 dB gain) to achieve 5 bps/Hz. Interestingly, the rate gain of FAS over TAS schemes is the most significant at medium SNR and it remains constant at high SNR. This suggests that the reconfiguration of FAS is more useful when the SNR is not at extreme values.

Figs. 3(a) and 3(b) show the individual rates of different schemes in the symmetric and asymmetric channel distributions, respectively.[5] In the asymmetric channel distribution, we assume that $\Omega_u = \frac{1}{u}, \forall u$. When compared to the same type of multiple access, each FAS user has a higher or similar rate than the same TAS user since the channel can be reconfigured to a more desirable one. Furthermore, NOMA schemes tend to allocate the remaining power to user 1 to improve the sum-rate after the user's rate requirement is satisfied. This is possible because all the degrees of freedom are shared among the users and the multi-user interference is canceled via SIC. In contrast, OMA schemes split the available degrees of freedom into U orthogonal channels to prevent multi-user interference. In such cases, waterfilling becomes essential to improve the sum-rate. Due to the orthogonal channels, the individual rates of OMA and OMAR remain similar in the symmetric case but they vary according to Ω_u in the asymmetric case. When CSIT is not available, both NOMA and waterfilling in OMA cannot be employed. Thus, evenly splitting the degrees of freedom and power allocation becomes a natural choice. Interestingly, this strategy is optimal if the channel distributions are symmetric but the optimality remains unclear in the asymmetric case.

[5]Note that the sum-rate in the asymmetric case has a similar trend as compared to the one in the symmetric case, see Fig. 2.

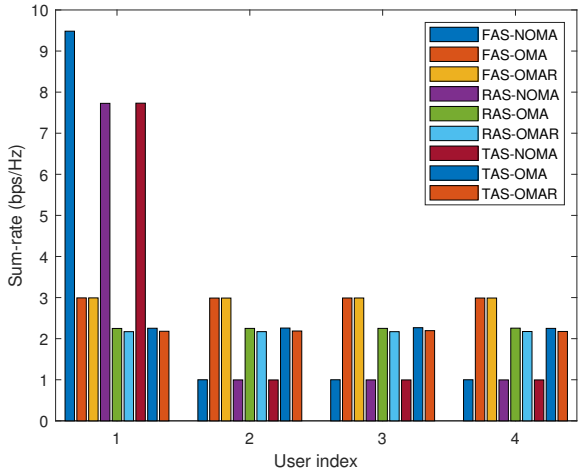

(a)

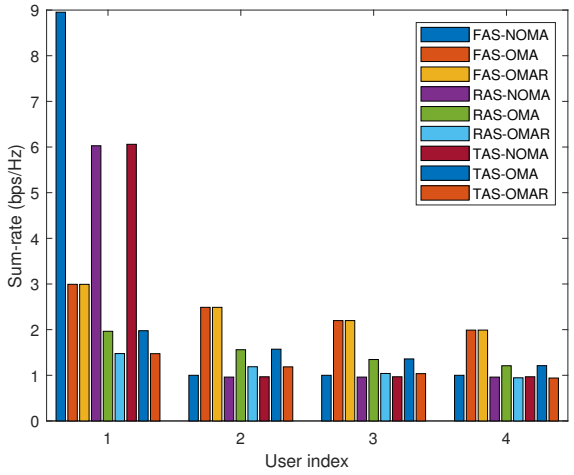

(b)

Figure 3: Individual rates of different schemes: a) symmetric and b) asymmetric channel distributions.

Figs. 4(a), 4(b) and 4(c) study the effects of N_{rx}, W_{rx} and U on different environments, respectively. In Fig. 4(a) we vary N^1_{rx} and fix $N^2_{\mathrm{rx}} = 10$. In Fig. 4(b), we vary W^1_{rx} and fix $W^2_{\mathrm{rx}} = 1$. We also consider two different environments: NLOS (solid lines) and LOS (dotted lines). In the LOS, we further assume that $K = 7$ and $L = 2$. As it is seen, the effects of N_{rx}, W_{rx} and U are more significant on the multiple access if the environment is NLOS. This means that FAS is more helpful in rich scattering situations. However, with LOS, reconfigurable intelligent surfaces can be employed along with FAS to create artificial scattering [15]. Moreover, it is noted that although the sum-rate may increase w.r.t. U, the average rate per user (i.e., the sum-rate divided by U) actually decreases. Therefore, all schemes are interference-limited (i.e., they can only support a limited number of users). In addition, there is a limit to the sum-rate improvement as N_{rx} and W_{rx} increase since the channel gains over a given area are correlated.

V. Conclusion

This letter investigated the applications of FAS in OMA and NOMA. In particular, we maximized the sum-rate of FAS-OMA and FAS-NOMA via optimal port selection and power allocation subject to per-user rate requirement. We then obtained the optimal variables in closed-form expressions. Compared to TAS, we showed that FAS either achieves a higher sum-rate for a fixed SNR or requires lower SNR to achieve a fixed sum-rate. Also, we illustrated that FAS without CSIT outperforms optimal TAS with CSIT. In addition, we highlighted that random port selection does not lead to any performance degradation here and FAS might be more useful in NLOS environments. Future works may consider the application of reconfigurable intelligent surfaces in FAS to improve the scattering effect in LOS environments.

References

[1] K.-K. Wong, K.-F. Tong, Y. Shen, Y. Chen, and Y. Zhang, "Bruce Lee-inspired fluid antenna system: Six research topics and the potentials for 6G," *Frontiers Commun. Netw.*, vol. 3, no. 853416, pp. 1–31, Mar. 2022.

[2] Y. Huang, L. Xing, C. Song, S. Wang, and F. Elhouni, "Liquid antennas: Past, present and future," *IEEE Open J. Antennas Propag.*, vol. 2, pp. 473–487, Mar. 2021.

[3] L. Tlebaldiyeva, G. Nauryzbayev, S. Arzykulov, A. Eltawil, and T. Tsiftsis, "Enhancing QoS through fluid antenna systems over correlated Nakagami-m fading channels," in *Proc. IEEE Wireless Commun. Netw. Conf. (WCNC)*, pp. 78–83, 10-13 Apr. 2022, Austin, TX, USA.

[4] M. Khammassi, A. Kammoun, and M.-S. Alouini, "A new analytical approximation of the fluid antenna system channel," *IEEE Trans. Wireless Commun.*, early access DOI:10.1109/TWC.2023.3266411.

[5] W. K. New, K.-K. Wong, H. Xu, K.-F. Tong, and C.-B. Chae, "Fluid antenna system: New insights on outage probability and diversity gain," *IEEE Trans. Wireless Commun.*, early access DOI:10.1109/TWC.2023.3276245.

[6] W. K. New, K.-K. Wong, X. Hao, K.-F. Tong, and C.-B. Chae, "An information-theoretic characterization of MIMO-FAS: Optimization, diversity-multiplexing tradeoff and q-outage capacity," *IEEE Trans. Wireless Commun.*, early access DOI:10.1109/TWC.2023.3327063.

[7] K.-K. Wong and K.-F. Tong, "Fluid antenna multiple access," *IEEE Trans. Wireless Commun.*, vol. 21, no. 7, pp. 4801–4815, Jul. 2022.

[8] Y. Liu *et al.*, "Developing NOMA to next generation multiple access: Future vision and research opportunities," *IEEE Wireless Commun.*, vol. 29, no. 6, pp. 120–127, Dec. 2022.

[9] H. Kong *et al.*, "Uplink multiple access with semi-grant-free transmission in integrated satellite-aerial-terrestrial networks," *IEEE J. Select. Areas Commun.*, vol. 41, no. 6, pp. 1723–1736, Jun. 2023.

[10] X. Mu, Z. Wang, and Y. Liu, "NOMA for integrating sensing and communications towards 6G: A multiple access perspective," *IEEE Wireless Commun.*, early access DOI:10.1109/MWC.015.2200559.

[11] W. K. New, C. Y. Leow, K. Navaie, and Z. Ding, "Robust non-orthogonal multiple access for aerial and ground users," *IEEE Trans. Wireless Commun.*, vol. 19, no. 7, pp. 4793–4805, Jul. 2020.

[12] C. Skouroumounis and I. Krikidis, "Fluid antenna with linear MMSE channel estimation for large-scale cellular networks," *IEEE Trans. Commun.*, vol. 71, no. 2, pp. 1112–1125, Feb. 2023.

[13] L. Zhu, W. Ma, B. Ning, and R. Zhang, "Movable-antenna enhanced multiuser communication via antenna position optimization," [Online] arXiv:2302.06978, 2023.

[14] L. Tlebaldiyeva, S. Arzykulov, T. A. Tsiftsis, and G. Nauryzbayev, "Full-duplex cooperative NOMA-based mmWave networks with fluid antenna system (FAS) receivers," in *Proc. Int. Balkan Conf. Commun. Netw. (BalkanCom)*, pp. 1–6, 5-8 Jun. 2023, Istanbul, Turkey.

[15] K.-K. Wong, K.-F. Tong, and C.-B. Chae, "Fluid antenna system–part III: A new paradigm of distributed artificial scattering surfaces for massive connectivity," *IEEE Commun. Lett.*, vol. 27, no. 8, pp. 1929–1933, Aug. 2023.

[16] K.-K. Wong, K.-F. Tong, and C.-B. Chae, "Fluid antenna system–part II: Research opportunities," *IEEE Commun. Lett.*, vol. 27, no. 8, pp. 1924–1928, Aug. 2023.

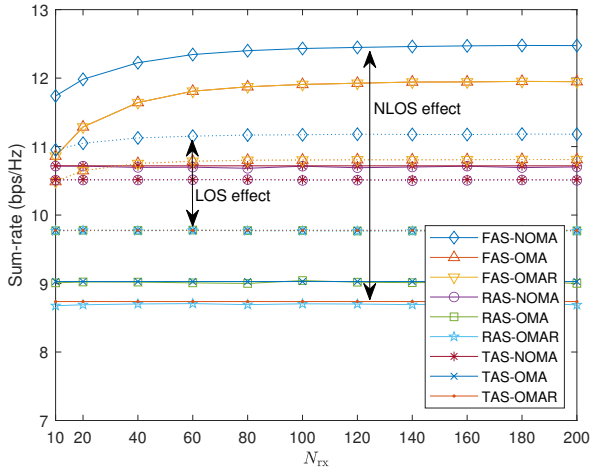

(a)

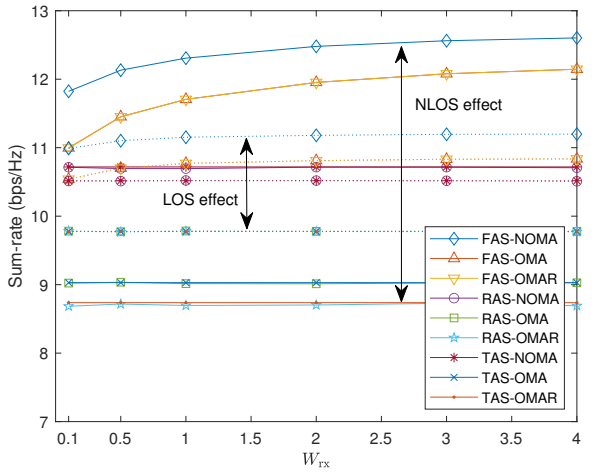

(b)

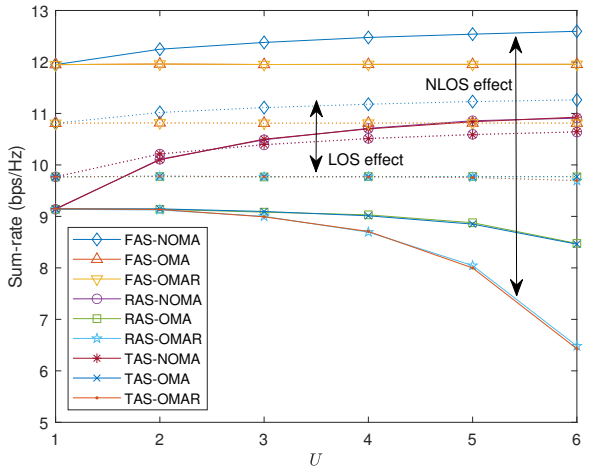

(c)

Figure 4: Effects of $N_{\rm rx}$, $W_{\rm rx}$ and U on different environments.